Title	Application of ball milling for highly selective mechanochemical polymorph transformations
Author(s)	Kamali, Naghmeh; Gniado, Katarzyna; McArdle, Patrick; Erxleben, Andrea
Publication Date	2018-06-07
Publication Information	Kamali, Naghmeh, Gniado, Katarzyna, McArdle, Patrick, & Erxleben, Andrea. (2018). Application of Ball Milling for Highly Selective Mechanochemical Polymorph Transformations. Organic Process Research & Development, 22(7), 796-802. doi: 10.1021/acs.oprd.8b00073
Publisher	American Chemical Society
Link to publisher's version	https://dx.doi.org/10.1021/acs.oprd.8b00073
Item record	http://hdl.handle.net/10379/14821
DOI	http://dx.doi.org/10.1021/acs.oprd.8b00073

Application of Ball Milling for Highly Selective Mechanochemical Polymorph Transformations

Naghmeh Kamali, Katarzyna Gniado, Patrick McArdle,* and Andrea Erxleben*
School of Chemistry, National University of Ireland, Galway, Ireland
*Corresponding author email address: andrea.erxleben@nuigalway.ie (AE);
p.mcardle@nuigalway.ie (PM)

For Table of Contents

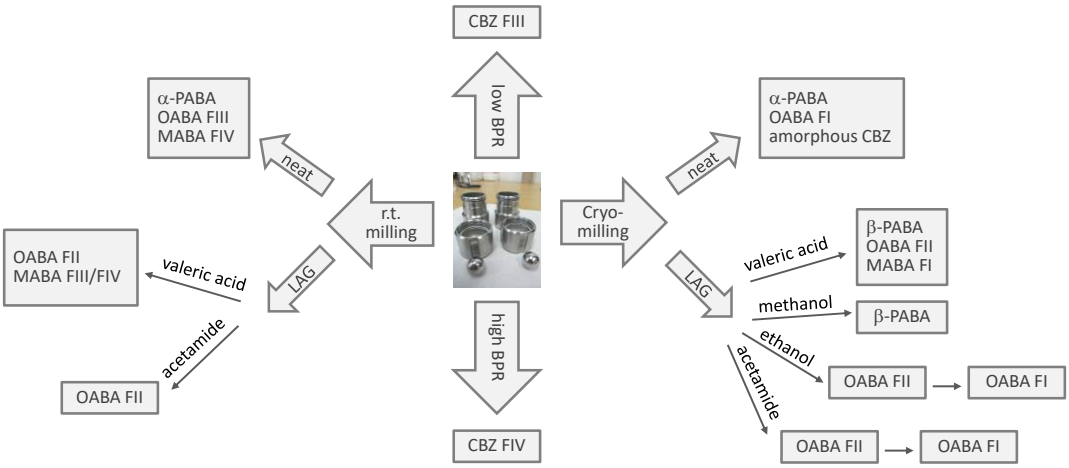

Abstract

Milling is an important secondary processing technique in the manufacture of pharmaceuticals, primarily used as a particle size reduction process. Para-, meta- and ortho-aminobenzoic acid (PABA, MABA, OABA) and carbamazepine (CBZ) are pharmaceutically relevant compounds that can exist in different polymorphic forms with distinct packing motifs and thus different physicochemical properties. A comprehensive study of the effect of milling on the polymorphism of PABA, MABA, OABA and CBZ was carried out. Milling PABA in the presence of catalytic amounts of valeric acid or methanol yielded the β-polymorph which is otherwise difficult to obtain in bulk quantities. Milling also proved to be a more convenient method for producing MABA form IV compared to previously reported procedures. Principal component analysis of the pair distribution function transformed X-ray powder diffraction spectra of ball-milled CBZ samples showed that the milling-induced polymorphic transformation strongly depends on the ball-to-powder ratio. Elusive CBZ form IV could be obtained in pure form by optimizing the milling conditions.

Keywords: amino benzoic acids, carbamazepine, milling, polymorphism, solid-state transformation

Introduction

Milling of powders is widely used in secondary pharmaceutical processing as a particle size reduction process. It can also be applied for the amorphization of crystalline solids,[1,2] mechanical alloying[3] and mechanochemical reactions.[4] The latter, in particular, is of interest as a solvent-free, *i.e.* 'green', method.

It is estimated that about 80 – 90 % of organic compounds are polymorphic, *i.e.* can crystallize in different forms with distinct packing and/or molecular conformations in the crystal lattice.[5] Different polymorphs differ in their physicochemical properties such as density, melting point, dissolution rate, chemical and physical stability, which in turn affect the processability, shelf-life and in the case of pharmaceuticals the bioavailability and thus the therapeutic efficacy.[6-9] Consequently, robust and reliable preparation methods for specific polymorphs are of utmost importance in process development. The most common approaches involve attempts to control the selective crystallization of the desired polymorph from solution through the careful development of the crystallization conditions (choice of solvent, cooling rate, supersaturation),[10,11] the use of tailor-made additives,[12] seeding,[13,14] or heteronucleation onto polymers.[14-16] However, in many cases batch-to-batch variability is an issue and often tedious and time-consuming screening experiments are required to find the optimum parameters. Alternatively, the desired solid-state form may be obtained through polymorphic

transformation. Mechanical and/or thermal stress, e.g. during grinding or milling, can lead to unintentional polymorphic conversions.[17-19] On the other hand, milling can be a convenient and green method for the deliberate generation of a specific polymorph through mechanochemically-induced solid-state transformation. Liquid-assisted or solvent-drop grinding, *i.e.* grinding in the presence of catalytic amounts of solvent, as a modification of neat grinding, can further enhance the efficiency of mechanochemical transformation. We have recently reported that milling of sulfathiazole form III in the presence of traces of solvent gives form IV with the phase purity strongly depending on the nature and the amount of the solvent.[20] In continuation of our work on milling-induced solid-state transformations we now show that ball-milling, both in the absence and in the presence of traces of solvent can achieve highly selective polymorph control in a number of cases. We present several examples where an (elusive) polymorph could be obtained that is not easily accessible in polymorphically pure form from solution.

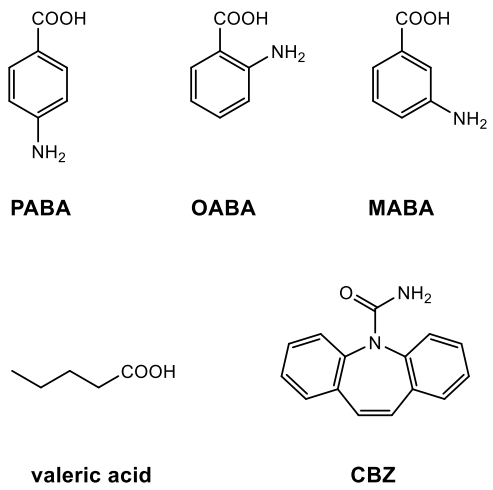

Figure 1. Chemical structures of PABA, OABA, MABA, valeric acid and CBZ.

Materials and Methods

Materials. *p*-aminobenzoic acid (PABA), *o*-aminobenzoic acid (OABA), *m*-aminobenzoic acid (MABA), carbamazepine (CBZ) and valeric acid (Figure 1) were purchased from Sigma-Aldrich. The polymorphic forms of the commercial samples were determined by X-ray powder diffraction (XRPD).

Ball milling. Room temperature milling experiments were performed in an oscillatory ball mill (Mixer Mill MM400, Retsch GmbH & Co., Germany) using a 25 mL stainless steel milling jar and one 15 mm diameter stainless steel ball. The samples (500 mg) were milled at 25 Hz for up to 150 min. with a cool down period of 15 min after every 30 min to prevent overheating of the samples. At

predetermined time intervals, the milled powder samples were analyzed by XRPD. For liquid-assisted grinding, 30 μL of the respective solvent was added to 500 mg powder prior to milling. Cryo-milling was carried out by immersing the milling jars initially in liquid nitrogen for 5 min. After every 7.5 min of milling the sample was cooled again in liquid nitrogen for 2.5 min. Milled samples were stored at ambient temperature and relative humidity (22 ± 2 ºC, 40 % RH) or ambient temperature and 85 % RH which was achieved in a desiccator using a saturated solution of KCl.[21] The polymorphic composition of the stored samples was monitored by XRPD.

Solution crystallization of β-form PABA. 3.0 g of PABA was dissolved in 30 mL of valeric acid, heated to 50 °C with stirring for 1 h and filtered. The filtrate was placed in a closed sample vial in a freezer at -20 °C overnight. The crystals were isolated by decanting the solvent. The XRPD pattern is shown in Figure S1 (Supporting Information).

X-ray powder diffraction (XRPD). X-ray powder patterns were recorded on an Inel Equinox 3000 powder diffractometer between 5 and 90 ° (2θ) using Cu K_α radiation (λ = 1.54178 Å, 35 kV, 25 mA). Theoretical powder patterns of the different polymorphs were calculated using the Oscail software package.[22]

Molecular orbital gas phase calculations. Molecular orbital DFT calculations were carried out using Gaussian 09 [23] using the B3LYP functional and 6-31G* basis sets. Molecules were constructed using Moilin within the Oscail package.[22]

Principal component analysis. Principal component analysis of the pair distribution function (PDF) transformed XRPD spectra of milled CBZ samples was carried out using the multivariate data analysis software The Unscrambler v.9.8 (Camo, Norway). The PDFgetX3 system was used for the PDF transformation.[24] The generation of the 2D input data files of XRPD data with first column and first row labels was automated within the Oscail software package.[22]

Results and Discussion

***p*-Aminobenzoic acid (PABA).** PABA (Figure 1) is used as a nutritional supplement and presents an important intermediate in the manufacture of dyes and pharmaceuticals.[25,26] It has three known polymorphs, α-form or FI (a = 18.551, b = 3.860, c = 18.642 Å, Z = 8; monoclinic, space group $P2_1/n$),[27] β-form or FIV (a = 6.275, b = 8.55, c = 12.80 Å, β = 108.30 °; Z = 4; monoclinic, space group $P2_1/c$),[28] and FV (a = 26.9945, b = 3.7322, c = 12.6731 Å; Z = 8; orthorhombic, space group $Pna2_1$).[29] The α- and β-forms are enantiotropically related, FV is a rare form that has only been obtained from an aqueous solution containing selenous acid[29] and by sublimation.[30] The β polymorph

is the stable form below the transition temperature of 13.8 °C,[31] while α-PABA is the commercial form and stable at room temperature. Crystallizing the pure β-form from solution has proved difficult and even at low temperature, where β-PABA is the more stable form, the two polymorphs tend to crystallize concomitantly.[10] Gracin and Rasmuson could obtain pure β-form from water and ethyl acetate by carefully controlling the temperature and supersaturation during cooling crystallization.[10] The structure of the α-form is based on carboxylic acid dimers involving strong H bonds (graph set notion $R_2^2(8)$), while the β-form contains four-membered rings with alternating amino- and carboxylic acid groups.[27,28] It was proposed that water which is a strong H bond acceptor and donor and ethyl acetate which is a strong H bond acceptor suppress the formation of carboxylic acid dimers in solution and thus allow the nucleation of the β polymorph.[10]

We found that the β-polymorph also crystallizes in pure form from valeric acid at -20 °C (Figure S1). It is reasonable to assume that the carboxylic acid interferes with the formation of PABA-PABA homodimers in solution and thus inhibits the nucleation of the α-form. We then investigated if bulk quantities of the β-form can be prepared mechanochemically by cryo-milling a commercial sample of α-PABA in the presence of valeric acid. The XRPD pattern of the sample cryo-milled with catalytic amounts of valeric acid for 90 min. showed indeed the complete conversion of the α-polymorph to the low temperature form (Figure 2). No transformation was observed during cryo-milling without added catalyst. Interestingly, the milling-induced α → β transformation was also observed when the highly corrosive valeric acid was replaced with the more benign solvent methanol (Figure 2). Both solvents have melting points lower than the milling temperature under cryo conditions. β-PABA obtained by liquid-assisted cryo-milling is stable for at least five months at room temperature and 85 % RH. On milling at room temperature for 10 min., in the absence of any solvent, the β-form converts back to the α-form. As expected, neat milling of α-PABA at room temperature did not lead to any changes in the XRPD pattern (Figure S1(e)).

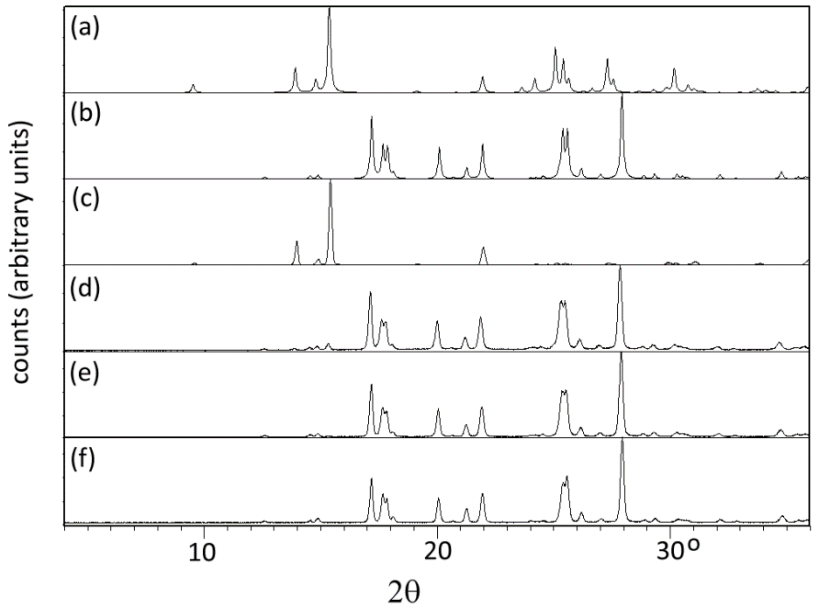

Figure 2. Measured and calculated XRPD patterns of PABA: (a) theoretical XRPD pattern of the α-form generated from single-crystal data (refcode: AMBNAC06), (b) theoretical XRPD pattern of the β-form generated from single-crystal data (refcode: AMBNAC04), (c) commercial sample, (d) commercial sample cryo-milled for 120 min. in the presence of valeric acid, (e) commercial sample cryo-milled for 90 min. in the presence of methanol, (f) commercial sample cryo-milled for 90 min. in the presence of methanol and stored for five months at 85 % RH.

o-Aminobenzoic acid (OABA). OABA, also known as anthralinic acid and vitamin L_1, has four polymorphs, FI (a = 12.868, b = 10.772, c = 9.325 Å, Z = 8, orthorhombic, space group $P2_1cn$),[32,33] FII (a = 15.973, b = 11.605, c = 7.162 Å, Z = 8, orthorhombic, space group Pbca),[34] FIIII (a = 6.537, b = 15.351, c = 7.086 Å, β = 112.64 °, Z = 4, monoclinic, space group $P2_1/c$)[35] and FIV (a = 4.9301, b = 11.2252, c = 11.5587 Å, β = 90.743 °, Z = 4, monoclinic, $P2_1/c$).[36] FII, FIII and FIV contain $R_2^2(8)$ carboxylic acid dimers. FI, the stable form at room temperature, has two molecules in the asymmetric unit, one ammonium/carboxylate zwitterion and one amino-carboxylic acid tautomer, that are alternately connected into a zigzag chain through COO^-···H-O and N^+-H···N hydrogen bonds.[33] FIII is the stable form at high temperature and can be obtained by melt crystallization or condensation from the gas phase.[37] Heating of FI and FII to 90 °C induces the transformation to FIII with FI converting faster than FII.[38] FI and FII crystallize concomitantly in antisolvent crystallization which was ascribed to competitive nucleation and growth.[39] ter Horst and coworkers showed that pure batches of all three polymorphs can be made by a combination of cooling crystallization and transformation. During cooling crystallization, initially pure FII crystallizes and then undergoes solvent-mediated transformations to FI and FIII at 45 and 60 °C, respectively.[11] The stability order FI

< FII < FIII was established for the 60 - 80 °C temperature range, while at lower temperature, the stability was suggested to increase in the order FII < FIII < FI.

As is evident from the XRPD pattern (Figure 3) the commercial sample used in our milling experiments is a mixture of FII and FIII. On milling at room temperature the Bragg peaks of FII disappear after 15 min and the XRPD pattern shows the presence of FIII only (Figure S2). When the sample is stored for nine days at ambient humidity (40% RH) some FII reappears. In the same time at 85% RH the XRPD pattern is close to the commercial pattern. It may be that undetectable seeds of FII, which had remained after milling, triggered the recrystallization of the metastable polymorph. Room temperature milling of the commercial form in the presence of valeric acid removes the Bragg peaks of FIII and the XRPD pattern shows only FII (Figure S3(e-g)). This sample was stable for five months at 85% RH. Milling in the presence of 10% acetamide gave similar results to milling in the presence of valeric acid (Figure S4). Cryo-milling leads to the conversion of the FII/FIII mixture to the low temperature polymorph FI. The time-dependent XRPD patterns (Figure S5) indicate that after 60 min FII has disappeared and after 150 min the Bragg peaks of FIII are no longer observed. It appears that FII converts to FIII and subsequently FIII converts to FI. FI obtained by cryo-milling is stable for at least five months at room temperature and 85 % RH. Cryo-milling for 60 min in the presence of valeric acid gave FII and no further changes were observed, when the milling was extended to 150 min (Figure S6). However, cryo-milling in the presence of ethanol gave FII after 30 min and after 90 min only FI was observed which was stable at 85% RH for five months (Figure 3). Similar results were obtained in the presence of 10% acetamide with the disappearance of FIII after 10 min when the XRPD corresponds to that of FII and after 60 min only FI is observed (Figure S6).

The transformation of the commercial FIII/FII mixture to FI on cryo-milling in the absence of solvent is interesting, as it requires the reorientation of the molecules as well as proton transfer to form the ammonium-carboxylate tautomer. We have discussed milling-induced transformations that involve charge separation in a previous paper.[40] Proton transfer under anhydrous, solvent-free conditions in the closed environment of a milling jar appears to be difficult and mechanochemical reactions between a carboxylic acid and a base in the absence of solvent seems to be limited to carboxylic acids with a melting point of less than 100 °C that may act in a solvent-like manner under milling conditions.[41] OABA has a melting point of 146 °C. Mechanical stress-induced intermolecular proton transfer between neutral piroxicam molecules (melting point 201 °C) was reported, but cryo-milling only gave 8 % conversion to the zwitterionic tautomer.[42] In the case of OABA the position of the amino group and carboxyl group ortho to each other can allow for a facile intramolecular proton transfer. Gas phase DFT calculations support this suggestion. Attempts to optimize the zwitterion structure of OABA led to proton transfer and the non-ionic OABA structure. The calculated energies for PABA, MABA and OABA indicate that MABA and OABA are 38 and 20 kJ mol^{-1} less stable than

PABA. It was also found that the zwitterion structures of PABA and MABA are 295 and 236 kJ mol^{-1} less stable than their non-ionized forms. The structures of these aminocarboxylic acids which contain zwitterions must clearly use some of their lattice energy to promote proton transfer.

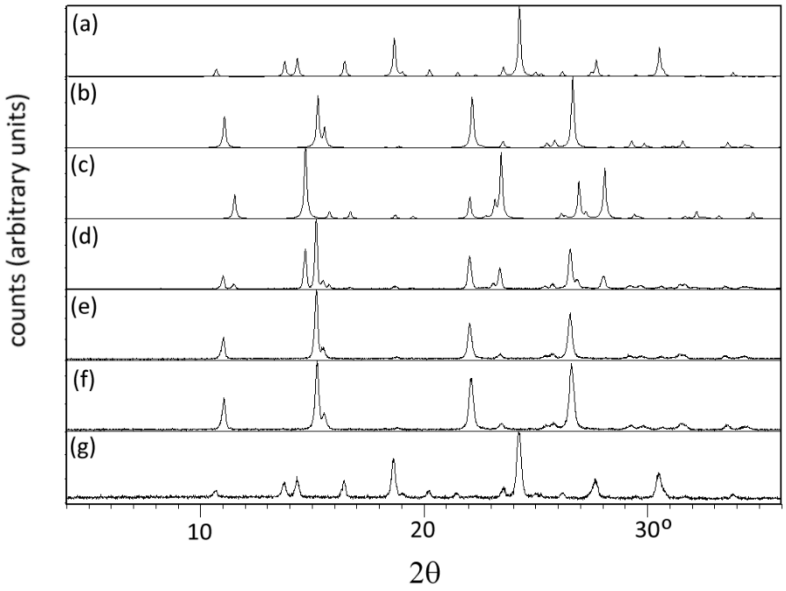

Figure 3. Measured and calculated XRPD patterns: (a) theoretical XRPD pattern of OABA FI generated from single-crystal data (refcode: AMBACO01), (b) theoretical XRPD pattern of OABA FII generated from single-crystal data (refcode: AMBACO05), (c) theoretical XRPD pattern of OABA FIII generated from single-crystal data (refcode: AMBACO08), (d) commercial sample, (e) commercial sample cryo-milled for 30 min. in the presence of ethanol, (f) commercial sample cryo-milled for 60 min. in the presence of ethanol and (g) commercial sample cryo-milled for 90 min. in the presence of ethanol.

m-Aminobenzoic acid (MABA). MABA belongs to the rare class of polymorphic systems that have at least five known polymorphs, FI (no crystal structure available),[43] FII (a = 5.047, b = 23.06, c = 11.790 Å, β = 105.47 °, Z' = 2, monoclinic, space group $P2_1/c$),[44] FIII (a = 21.3393, b = 7.29604, c = 3.77733 Å, β = 94.8240 °, Z = 4, monoclinic, space group $P2_1/a$),[45] FIV (a = 3.80003, b = 11.55389, c = 14.6333 Å, α = 110.5047, β = 92.7424 °, γ = 96.5930, Z = 2, triclinic, space group $P\bar{1}$),[45] and FV (a = 14.7870, b = 4.95659, c = 9.0814 Å, β = 95.2119 °, Z = 4, monoclinic, space group $P2_1/a$).[45] In FI, FIII and FIV MABA adopts the zwitterionic form, while in FII and FV the molecules exist in the non-zwitterionic form. Three polymorphs, FIII – FV, were only identified in 2012 [45] and

there is still no certainty about the stability order of all polymorphs. The densities of the polymorphs whose structure has been determined from single crystal X-ray or powder data suggest the order FIII > FIV >> FII > FV.[45]

The XRPD pattern of the commercial form shows the Bragg peaks specific to FIII. On milling at room temperature the formation of FIV is observed (Figure 4). In contrast to the transformations of OABA and PABA, the broad peaks observed at the early stages suggest that the transformation proceeds via a transient amorphous phase. The transformation is complete after 60 min and milling for up to 120 min does not result in any further changes except for a sharpening of the initially broad peaks. Form IV obtained this way is stable for at least five months at ambient temperature and 85 % RH. FIV was first identified in a DSC experiment, by melting FIII followed by cooling to room temperature in a sealed aluminium pan and was also obtained by sublimation and condensation onto a glass cold finger.[45] The neat milling-induced FIII → FIV transformation seems to present a more convenient method for producing bulk quantities of this polymorph. Some form IV also forms, when traces of valeric acid are added prior to the milling (Figure S7). The peaks of FIV increase in intensity during the first 90 min of milling. In contrast to the neat milling experiment, in this case the FIII/FIV mixture obtained after 90 min appears to be the end-product. The reverse *i.e.* room temperature milling of FIV in the presence of valeric acid gave the same mixture of FIII and FIV. The crystal structures of FIII and FIV that were solved from powder data show similar packing motifs with bilayers of zwitterionic MABA molecules. In both cases the NH_3^+ groups are in H bonding distance to four neighbouring COO^- groups. The aryl rings form the upper and lower surfaces of the bilayers adopting different orientations in FIII and FIV. The similarity in the packing motifs should facilitate the interconversion between the two polymorphs. However, cryo-milling FIII with valeric acid gave FI. This FI sample stored at room temperature transformed to FIII after 3 days (Figure S8).

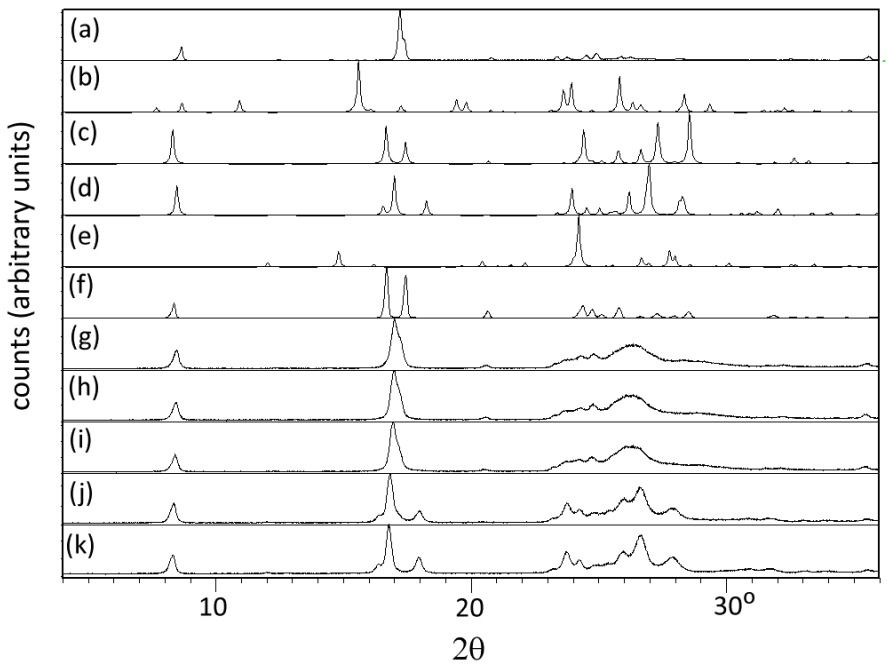

Figure 4. Measured and calculated XRPD patterns: (a) XRPD pattern of MABA FI, (b) theoretical XRPD pattern of MABA FII generated from single-crystal data (refcode: AMBNZA), (c) theoretical XRPD pattern of MABA FIII generated from refcode: AMBNZA01, (d) theoretical XRPD pattern of MABA FIV generated from refcode: AMBNZA02, (e) theoretical XRPD pattern of MABA FV generated from single-crystal data (refcode: AMBNZA03), (f) commercial sample, (g) – (k) commercial sample milled for 5, 15, 30, 60, and 120 min. at room temperature.

Carbamazepine (CBZ). The anti-epileptic drug CBZ is another example for a pharmaceutically relevant compound with a complicated polymorphism. Five polymorphs are known, forms FI – FV (FI: a = 5.1705 Å, b = 20.574 Å, c = 22.245 Å, α = 84.12 °, β = 88.01 °, γ = 85.19 °, triclinic, space group $P\bar{1}$;[46] FII: a = 35.454 Å, c = *5.253* Å, α = 90 °, β = 90 °, γ = 120 °, trigonal, space group $R\bar{3}$;[47] FIII: a = 7.529 Å, b = 11.148 Å, c = 15.470 Å, β = 116.17 °, monoclinic, space group $P2_1/c$;[48] FIV: a = 26.609 Å, b = 6.9269 Å, c = 13.957 Å, β = 109.702 °, monoclinic, space group C2/c;[12] FV: a = 9.1245 Å, b = 10.4518 Å, c = 24.8224 Å, orthorhombic, space group Pbca[49]) with the reported stability order FIII > FI > FIV > FII.[14] CBZ is poorly soluble in water and its dissolution-limited absorption and bioavailability strongly depend on the polymorphic form.[50] Metastable FIV was originally discovered in solution crystallization experiments in the presence of hydroxypropylcellulose, when it crystallized concomitantly with FIII and FI.[12] Later, other polymers (poly(4-methylpentene), poly(R-methylstyrene), and poly(p-phenylene ether-sulfone)) were also shown to encourage the crystallization of FIV.[15] It was reported that seeding supersaturated methanol solutions produced FIV which, however, was occasionally contaminated with FI.[14] Subsequent attempts to crystallize FIV from solution in the absence of templates were unsuccessful[51,52] and it was proposed that this polymorph transforms rapidly to the more stable FI or FIII through solution-mediated transformation. Harris *et al*. reported the preparation of FIV by drying CBZ·$2H_2O$ over P_2O_5.[53] Recently, Halliwell *et al*. showed that polymorphically pure FIV can be reproducibly obtained by spray-drying of methanolic CBZ solutions.[54] The stability order FIII > FI > FIV > FII[14] suggests that the elusive polymorph FIV may be accessible *via* ball-milling. The amorphization of CBZ by milling FIII in the presence of excipients has been described.[55,56] Using our standard milling parameters (0.5 to 1 g powder, 25 cm^3 milling jar, 15-mm ball, 25 Hz) we observed little change in the XRPD pattern of the milled samples (Figure S9). Milling under cryo conditions gave largely amorphous CBZ (Figure S10). However, when the ball-to-powder ratio was increased, FIV could be detected in the XRPD patterns. Different quantities of CBZ FIII were milled at room temperature for a range of times and a principal component analysis (PCA) of the pair distribution function (PDF) transformed XRPD spectra was carried out. The use of PDF to improve PCA of even XRPD data obtained with Cu radiation has been previously described.[57] The PCA explained 88% of the variance

of the data before application of the PDF transformation, Figure S11, and 97 % of the variance after transformation. The evolution of FIV (Figure 5) is also clearer after the PDF transformation and the amount of FIV produced was proportional to the milling time and inversely proportional to the quantity milled. Milling 125 mg CBZ FIII for 90 min yielded pure FIV. The use of one 15-mm milling ball was found to be crucial. When the milling was carried out with two to ten 5-mm balls, the XRPD patterns showed the presence of FIII with an underlying amorphous halo. Examination of the XRPD patterns suggests that the only forms observed during the form III to form IV transformation were forms III and IV. The effect of ball-to-powder ratio has been discussed in the literature.[58,59] During ball-milling high energies are generated with the energy conditions in the milling jar being determined by the frequency of stress events and the stress energy transferred to the powder at each impact. The lower the amount of powder, the higher the velocity and thus the kinetic energy of the ball(s) and the higher the stress energy transferred from the ball(s) to the powder. The ball-to-powder ratio also determines the final particle size and thus the effective surface area. The size of the surface area is important as molecules at the surface have a higher mobility than molecules inside the particle. Given the suggested stability order ball milling with a high ball to powder ratio is a relatively high energy process and CBZ is transformed past FI to form IV. It is possible that the stability of solvent channel void containing form II in the absence of a solvent is very low under the conditions in the ball mill.

The milling-induced solid-state transformations are reminiscent of the classical Viedma ripening experiment in which crystals subjected to magnetic stirring were continuously crushed by small glass balls.[60] This led to a continuous enhancement of crystal enantiomeric excess in a saturated solution containing D and L crystals of $NaClO_3$ through a nonlinear autocatalytic recycling process. Fragments broken off the crystal surface are recycled and feed larger crystals when they are at a sub-unit cell level and have lost all crystal information. The number of glass balls and speed of agitation determine the time required to achieve complete chiral purity. It was pointed out that mechanical abrasion grinding of crystals by glass balls works like a mill[60] and there is some analogy in abrasion-grinding induced deracemization and polymorph selectivity and phase purity obtained by milling.

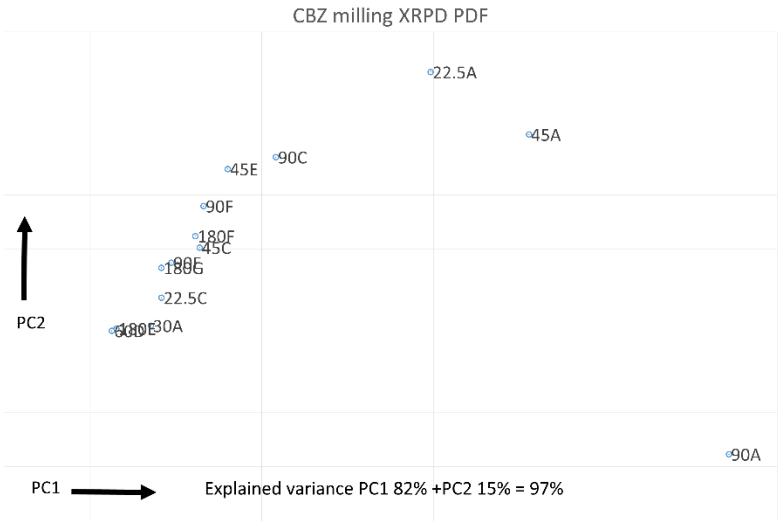

Figure 5. PCA analysis of CBZ form III milling. The points are labelled with milling time in mins and the quantities used were: A, 125; B, 167; C, 250; D, 333; E, 500; F, 1000; and , 2000 mg.

Conclusions

Milling can present a convenient, robust and 'green' method for the preparation of polymorphs. Through the right choice of milling conditions and the use of additives or catalytic amounts of solvent OABA FI, OABA FII, MABA FI, MABA FIV and elusive and difficult to obtain CBZ FIV and β-PABA can be selectively and reliably produced. The study thus further illustrates the advantages and potential of mechanochemical processes.

Supporting Information Available

Additional XRPD patterns

Acknowledgement

This work was supported by Science Foundation Ireland under Grant No. [12/RC/2275] as part of the Synthesis and Solid State Pharmaceutical Centre (SSPC).). The Irish Centre for High-End Computing, ICHEC, is thanked for the provision of computational resources to project ngche046c.

References

(1) Caron, V.; Willart, J. F.; Lefort, R.; Derollez, P.; Danede, F.; Descamps, M. Solid state amorphization kinetic of alpha lactose upon mechanical milling. *Carbohydr. Res*. **2011**, *346*, 2622–2628.

(2) Karmwar, P.; Graeser, K.; Gordon, K. C.; Strachan, C. J., Rades, T. Effect of different preparation methods on the dissolution behaviour of amorphous indomethacin. *Eur. J. Pharm. Biopharm*. **2012**, *80*, 459–464.

(3) Suryanarayana, C. Mechanical alloying and milling. *Prog. Mater. Sci.* **2001**, *46*, 1–184.

(4) Friščić, T.; Jones, W. Recent advances in understanding the mechanism of cocrystal formation via grinding. *Cryst. Growth Des*. **2009**, *9*, 1621–1637.

(5) Stahly, G. P. Diversity in Single- and Multiple-Component Crystals. The search for and prevalence of polymorphs and cocrystals. *Cryst Growth Des*. **2007**, *7*, 1007–1026.

(6) Haleblian, J.; McCrone, W. Pharmaceutical applications of polymorphism. *J. Pharm. Sci*. 1**969**, *58*, 911–929.

(7) Raw, A. S.; Yu, L. X. Pharmaceutical solid polymorphism in drug development and regulation. *Adv. Drug Deliv. Rev*. **2004**, *56*, 235–236.

(8) Datta, S.; Grant, D. J. W. Crystal structures of drugs: advances in determination, prediction and engineering. *Nat. Rev. Drug Discov*. **2004**, *3*, 42–57.

(9) Llinàs, A.; Goodman, J. M. Polymorph control: past, present and future. *Drug Discov. Today* **2008**, *13*, 198–210.

(10) Gracin, S.; Rasmuson, A. Polymorphism and crystallization of p-aminobenzoic acid. *Cryst. Growth Des*. **2004**, *4*, 1013–1023.

(11) Jiang, S.; Jansens, P. J.; ter Horst, J. H. Control over polymorph formation of o-aminobenzoic acid. *Cryst. Growth Des*. **2010**, *10*, 2541–2547.

(12) Lang, M.; Kampf, J. W.; Matzger, J. Form IV of carbamazepine. *J. Pharm. Sci*. **2002**, *91*, 1186–1190.

(13) Nichols, G.; Frampton, C. S. Physicochemical characterization of the orthorhombic polymorph of paracetamol crystallized from solution. *J. Pharm. Sci.* **1998**, *87*, 684–693.

(14) Crzesiak, A. L.; Lang, M.; Kim, K.; Matzger, A. J. Comparison of the four anhydrous polymorphs of carbamazepine and the crystal structure of form I. *J. Pharm. Sci*. **2003**, *92*, 2260–2271.

(15) Lang, M.; Grzesiak, A. L.; Matzger, A. J. The use of polymer heteronuclei for crystalline polymorph selection. *J. Am. Chem. Soc.* **2002**, *124*, 14834–14835.

(16) Lopez-Mejias, V.; Kampf, J. W.; Matzger, A. J. Nonamorphism in flufenamic acid and a new record for a polymorphic compound with solved structures. *J. Am. Chem. Soc*. **2012**, *134*, 9872–9875.

(17) Lin, S. Y.; Hsu, C. H.; Ke, W. T. Solid-state transformation of different gabapentin polymorphs upon milling and co-milling. *Int. J. Pharm*. **2010**, *396*, 83–90.

(18) Lin, S. Y.; Cheng, W. T.; Wang, S. L. Thermodynamic and kinetic characterization of polymorphic transformation of famotidine during grinding. *Int. J. Pharm*. **2006**, *318*, 86–91.

(19) Chieng, N.; Zujovic, Z.; Bowmaker, G.; Rades, T.; Saville, D. Effect of milling conditions on the solid-state conversion of ranitidine hydrochloride form 1. *Int. J. Pharm*. **2006**, *327*, 36–44.

(20) Hu, Y.; Erxleben, A.; Hodnett, B. K.; Li, B.; McArdle, P.; Rasmuson, Å. C.; Ryder, A. G. Solid-state transformations of sulfathiazole polymorphs: The effects of milling and humidity. *Cryst. Growth Des*. **2013**, *13*, 3404–3413.

(21) Lu, T.; Chen, C. Uncertainty evaluation of humidity sensors calibrated by saturated salt solutions. *Measurement* **2007**, *40*, 591–599.

(22) McArdle, P. Oscail, a program package for small-molecule single-crystal crystallography with crystal morphology prediction and molecular modelling. *J. Appl. Crystallogr*. **2017**, *50*, 320–326.

(23) Frisch, M. J.; Trucks, G. W.; Schlegel, H. B.; Scuseria, G. E.; Robb, M. A.; Cheeseman, J. R.; Scalmani, G.; Barone, V.; Mennucci, B.; Petersson, G. A.; Nakatsuji, H.; Caricato, M.; Li, X.; Hratchian, H. P.; Izmaylov, A. F.; Bloino, J.; Zheng, G.; Sonnenberg, J. L.; Hada, M.; Ehara, M.; Toyota, K.; Fukuda, R.; Hasegawa, J.; Ishida, M.; Nakajima, T.; Honda, Y.; Kitao, O.; Nakai, H.; Vreven, T.; Montgomery, A. J.; Peralta, J. E.; Bearpark, M.; Heyd, J. J.; Brothers, E.; Kudin, K. N.; Staroverov, V. N.; Kobayashi, R.; Normand, J.; Raghavachari, K.; Rendell, A.; Burant, J. C.; Iyengar, S. S.; Tomasi, J.; Cossi, M.; Rega, N.; Millam, J. M.; Klene, M.; Knox, J. E.; Cross, J. B.; Bakken, V.; Adamo, C.; Jaramillo, J.; Gomperts, R.; Stratmann, R. E.; Yazyev, O.; Austin, A. J.; Cammi, R.; Pomelli, C.; Ochterski, J. W.; Martin, R. L.; Morokuma, K.; Zakrzewski, V. G.; Voth, G. A.; Salvador, P.; Dannenberg, J. J.; Dapprich, S.; Daniels, A. D.; Farkas, Ö.; Foresman, J. B.; Ortiz, J. V.; Cioslowski, J.; Fox, D. J. *Gaussian 09, Revision B.01*, Gaussian, Inc.: Wallingford CT, USA, 2009.

(24) Juhas, P.; Davis, T.; Farrow, C. L.; Billinge, S. J. L. PDFgetX3: a rapid and highly automatable program for processing powder diffraction data into total scattering pair distribution functions. *J. Appl. Crystallogr.* **2013**, *46*, 560–566.

(25) Tripathi, G. N. R.; Su, Y. Spectroscopic and kinetic properties of the radical zwitterion and related intermediates in the one-electron oxidation of p-aminobenzoic Acid. *J. Am. Chem. Soc*. **1996**, *118*, 2235–2244.

(26) Chignell, C. F.; Kalynaraman, B.; Mason, R. P.; Sik, R. H. Spectroscopic studies of cutaneous photosensitizing agents-I. Spin trapping of photolysis products from sulfanilamide, 4-aminobenzoic acid and related compounds. *Photochem. Photobiol*. **1980**, *32*, 563–571.

(27) Lai, T. F.; Marsh, R. E. The crystal structure of p-aminobenzoic acid. *Acta Crystallogr*. **1967**, *22*, 885–893.

(28) Gracin, S.; Fischer, A. Redetermination of the beta-polymorph of p-aminobenzoic acid. *Acta Crystallogr*. **2005**, *E61*, o1242–o1244.

(29) Benali-Cherif, R.; Takouachet, R.; Bendeif, E.-E.; Benali-Cherif, N. The structural properties of a noncentrosymmetric polymorph of 4-amino-benzoic acid. *Acta Cryst. C* **2014,** *70*, 323–325.

(30) Kamali, N.; Erxleben, A.; McArdle, P. Unexpected effects of catalytic amounts of additives on crystallization from the gas phase: Depression of the sublimation temperature and polymorph control. *Cryst. Growth Des.* **2016**, *16*, 2492–2495.

(31) Hao, H.; Barrett, M.; Hu, Y.; Su, W.; Ferguson, S.; Wood, B.; Glennon, B. The use of in situ tools to monitor the enantiotropic transformation of p-aminobenzoic acid polymorphs. *Org. Process Res. Dev*. **2012**, *16*, 35–41.

(32) Brown, C. J. Crystal structure of anthranilic acid. *Proc. R. Soc. London, Ser. A* **1968**, *302*, 185–199.

(33) Brown, C. J.; Ehrenberg, M. Anthranilic acid, $C_7H_7NO_2$, by neutron diffraction. *Acta Crystallogr., Sect. C: Cryst. Struct. Commun*. **1985**, *41*, 441–443.

(34) Boone, C. D. G.; Derissen, J. L.; Schoone, J. C. Anthranilic acid II (o-aminobenzoic acid). *Acta Crystallogr., Sect. B: Struct. Crystallogr. Cryst. Chem*. **1977**, *33*, 3205–3206.

(35) Takazawa, H.; Ohba, S.; Saito, Y. Structure of monoclinic o-aminobenzoic acid. *Acta Crystallogr., Sect. C: Cryst. Struct. Commun*. **1986**, *42*, 1880–1881.

(36) Lu, T.-H.; Chattopadhyay, P.; Liao, F.-L.; Lo, J.-M. Crystal structure of 2-aminobenzoic acid. *Anal. Sci.* **2001**, *17*, 905–906.

(37) Ojala, W. H.; Etter, M. C. Polymorphism in anthranilic acid: a reexamination of the phase transitions. *J. Am. Chem. Soc*. **1992**, *114*, 10288–10293.

(38) Jiang, S.; Jansens, P.; ter Horst, J. H. Mechanism and kinetics of the polymorphic transformation of o-aminobenzoic acid. *Cryst. Growth Des*. **2010**, *10*, 2123–2128.

(39) Jiang, S.; ter Horst, J. H.; Jansens, P. J. Concomitant polymorphism of o-aminobenzoic acid in antisolvent crystallization. *Cryst. Growth Des*. **2008**, *8*, 37–43.

(40) Hu, Y.; Gniado, K.; Erxleben, A.; McArdle, P. Mechanochemical reaction of sulfathiazole with carboxylic acids: Formation of a cocrystal, a salt and coamorphous solids. *Cryst. Growth Des*. **2014,** *14*, 803–813.

(41) Trask, A. V.; Haynes, D. A.; Motherwell, W. D. S.; Jones, W. Screening for crystalline salts via mechanochemistry. *Chem. Commun*. **2006**, *1*, 51–53.

(42) Sheth, A. R.; Lubach, J. W.; Munson, E. J.; Muller, F. X.; Grant, D. J. W. Mechanochromism of piroxicam accompanied by intermolecular proton transfer probed by spectroscopic methods and solid-phase changes. *J. Am. Chem. Soc.* **2005**, *127*, 6641-6651.

(43) Theoret, A. Structure moléculaire et zwitterion des acides aminés—I. Spectres infrarouges des acides o, m et p-aminobenzoïques dans différentes formes cristallines. *Spectrochim. Acta* **1971**, *27A*, 11–18.

(44) Voogd, J.; Verzijl, B. H. M.; Duisenberg, A. J. M. m-Aminobenzoic acid. *Acta Crystallogr., Sect. B: Struct. Sci*. **1980**, *36*, 2805–2806.

(45) Williams, P. A.; Hughes, C. E.; Lim, G. K.; Kariuki, B. M.; Harris, K. D. M. Discovery of a new system exhibiting abundant polymorphism: m-Aminobenzoic acid. *Cryst. Growth Des*. **2012**, *12*, 3104–3113.

(46) Grezsiak A. L.; Lang, M.; Kim, K.; Matzger, A. J. Comparison of the four anhydrous polymorphs of carbamazepine and the crystal structure of form I. *J. Pharm. Sci*. **2003**, *92*, 2260–2271.

(47) Lowes, M. M.; Caira, M. R.; Lötter, A. P.; van der Watt, J. G. Physicochemical properties and X-ray structural studies of the trigonal polymorph of carbamazepine. *J. Pharm. Sci*. **1987**, *76*, 744–752.

(48) Reboul, J. P.; Cristou, B.; Soyfer, J. C.; Astier, J. P. 5H-Dibenz[b,f]azépinecarboxamide-5 (carbamazépine). *Acta Crystallogr. Sect. B Struct. Sci*. **1981**, *37*, 1844–1848.

(49) Arlin, J.-B.; Price, L. S.; Price, S. L.; Florence, A. J. A strategy for producing predicted polymorphs: catemeric carbamazepine form V. *Chem. Commun*. **2011**, *47*, 7074–7076.

(50) Kobayashi, Y.; Ito, S.; Itai, S.; Yamamoto, K. Physicochemical properties and bioavailability of carbamazepine polymorphs and dihydrate. *Int. J. Pharm*. **2000**, *193*, 137–146.

(51) Florence, A. J.; Johnston, A.; Price, S. L.; Nowell, H.; Kennedy, A. R.; Shankland, N. An automated parallel crystallisation search for predicted crystal structures and packing motifs of carbamazepine. *J. Pharm. Sci*. **2006**, *95*, 1918–190.

(52) Getsoian, A.; Lodaya, R. M.; Blackburn, A. C. One-solvent polymorph screen of carbamazepine. *Int. J. Pharm*. **2008**, *348*, 3–9.

(53) Harris, R.; Ghi, P. Y.; Puschmann, H.; Apperley, D. C.; Griesser, U.; Hammond, R.; Ma, C.; Roberts, K. J.; Pearce, G. J.; Yates. J. R.; Pickard, C. J. Structural studies of the polymorphs of carbamazepine, its dihydrate, and two solvates. *Org. Process Res. Dev*. **2005**, *9*, 902–910.

(54) Halliwell, R. A.; Bhardwaj, R. M.; Brown, C. J.; Briggs, N. E. B.; Dunn, J.; Robertson, J.; Nordon, A.; Florence, A. J. Spray drying as a reliable route to produce metastable carbamazepine form IV. *J. Pharm. Sci*. **2017**, *106*, 1874–1880.

(55) Löbmann, K.; Grohganz, H.; Laitinen, R.; Strachan, C.; Rades, T. Amino acids as co-amorphous stabilizers for poorly water soluble drugs–Part 1: preparation, stability and dissolution enhancement. *Eur. J. Pharm. Biopharm*. **2013**, *85*, 873–881.

(56) Gniado, K.; MacFhionnghaile, P.; McArdle, P.; Erxleben, A. The natural bile acid surfactant sodium taurocholate (NaTC) as a coformer in coamorphous systems: Enhanced physical stability and dissolution behavior of coamorphous drug-NaTc systems. *Int. J. Pharm*. **2018**, *535*, 132–139.

(57) Bøtker, J. P.; Karmwar, P.; Strachan, C. J.; Cornett, C.; Tian, F.; Zujovic, Z.; Rantanen, J.; Rades, T. Assessment of crystalline disorder in cryo-milled samples of indomethacin using atomic pair-wise distribution functions. *Int. J. Pharm.* **2011**, *417*, 112–119.

(58) Kulla, H.; Fischer, F.; Benemann, S.; Rademann, K.; Emmerling; F. The effect of the ball to reactant ratio on mechanochemical reaction times studied by in situ PXRD. *CrystEngComm*. **2017**, *19*, 3902–3907.

(59) Pazesh, S.; Gråsjö, J.; Berggren, J.; Alderborn, G. Comminution-amorphisation relationships during ball milling of lactose at different milling conditions. *Int. J. Pharm*. **2017**, *528*, 215–227.

(60) Viedma, C. Chiral symmetry breaking during crystallization: Complete chiral purity induced by nonlinear autocatalysis and recyclic. *Phys. Rev. Lett*. **2005**, *94*, 065504.